Crossover from two- to three-dimensional critical behavior for nearly antiferromagnetic itinerant electrons.

Anne-Marie Daré, Y.M.Vilk, and A.-M.S. Tremblay
Département de physique and Centre de recherche en physique du solide.
Université de Sherbrooke, Sherbrooke, Québec, Canada J1K 2R1
(17 January 1996, cond-mat/9602083)

The crossover from two- to three-dimensional critical behavior of nearly antiferromagnetic itinerant electrons is studied in a regime where the inter-plane single-particle motion of electrons is quantum-mechanically incoherent because of thermal fluctuations. This is a relevant regime for very anisotropic materials like the cuprates. The problem is studied within the Two-Particle Self-Consistent approach (TPSC), that has been previously shown to give a quantitative description of Monte Carlo data for the Hubbard model. It is shown that TPSC belongs to the $n \to \infty$ limit of the $O(n)$ universality class. However, contrary to the usual approaches, cutoffs appear naturally in the microscopic TPSC theory so that parameter-free calculations can be done for Hubbard models with arbitrary band structure. A general discussion of universality in the renormalized-classical crossover from $d = 2$ to $d = 3$ is also given.

PACS numbers: 75.10.Lp, 71.27.+a, 71.10.+x, 74.72.-h

arXiv:cond-mat/9602083v1 15 Feb 1996

I. INTRODUCTION

A simple model of itinerant antiferromagnets is provided by electrons on a lattice with short-range repulsion. In the low temperature phase, the system is in a Spin Density Wave (SDW) state. In three dimensions, above the transition temperature, the electrons form a so-called *nearly antiferromagnetic Fermi liquid*. Traditional mean-field techniques for studying SDW instabilities of Fermi liquids fail completely in low dimension. In two dimensions for example, the Random Phase Approximation (RPA) predicts finite temperature antiferromagnetic transitions while this is forbidden by the Mermin-Wagner theorem. Nevertheless, one can study universal critical behavior using various forms of renormalization group treatments appropriate either for the strong [1] [2] [3] or the weak-coupling limits [4] [5]. The self-consistent-renormalized approach of Moryia [6] also satisfies the Mermin-Wagner theorem in two dimensions. Since cutoff-dependent scales are left undetermined by all these approaches they must be found by other methods. For example, in the strong-coupling limit, the spin-stiffness constant of the non-linear $\sigma-$model must be determined from Monte Carlo simulations. In the weak-coupling case however, Monte Carlo simulations are limited to very small systems, of order 10×10 that do not allow one to study much of the critical regime.

Recently, the Two-Particle Self-Consistent approach [7] was developed to obtain from a microscopic model a *quantitative* description of itinerant electrons not only far from phase transitions, but also in the critical regime. It was shown [7] that in this approach the Mermin-Wagner theorem is satisfied and that, away from the critical regime, the approach gives quantitative agreement with Monte Carlo simulations of the nearest-neighbor [7] and next-nearest neighbor [8] Hubbard model in two dimensions. Quantitative agreement is also obtained as one enters the narrow critical regime accessible in Monte Carlo simulations. The approach is restricted to the one-band Hubbard model with on-site interaction, but is valid for arbitrary dispersion relation. The TPSC approach also allows one to study the case where the instability of the itinerant electrons is at an incommensurate wave-vector, but in this paper we restrict ourselves to the case where the order is at the antiferromagnetic wave vector. The self-consistent-renormalized approach of Moryia [6] cannot deal with the incommensurate case without *a priori* information. Even though it has the same critical behavior as the TPSC approach it does not allow one to obtain quantitative parameter-free results from a microscopic Hamiltonian.

We first show in full generality that the TPSC approach gives the leading term of the critical behavior in a $1/n$ expansion. In other words, it gives the $n \to \infty$ limit of the $O(n)$ model where $n = 3$ is the physically correct (Heisenberg) limit. It will be apparent that there is no arbitrariness in cutoff so that, given a microscopic Hubbard model, no parameter is left undetermined. One can go with the same theory from the non-critical to the critical regime.

We then show that the previously studied two-dimensional critical regimes, namely quantum-critical [2] and renormalized classical [1] are reproduced here to leading order in $1/n$. In the quantum critical regime, one usually distinguishes two cases [2]: Model A, where the paramagnetic Fermi surface does not intersect the magnetic Brillouin zone, and Model B where it does. This distinction is important in the quantum critical regime because it changes the

dynamical critical exponent. In this paper, we also give results on Model C, the case of perfect nesting. In this case, the microscopic approach shows that modifications to frequency-independent thermodynamic properties can arise. In particular, in the two-dimensional perfect-nesting case the usual exponential dependence of correlation length on temperature $\exp(cst/T)$ can be modified to be roughly $\exp\left(cst/T^3\right)$ in some temperature region of the renormalized classical regime.

Then we study the renormalized-classical crossover from $d = 2$ to $d = 3$ in the highly anisotropic case of weakly coupled planes. [9] The general theory of such crossover is given in Appendix D, along with a discussion of universal crossover functions. In the main text it is shown that in the highly anisotropic case the crossover can occur in a rather unusual regime, namely $t_\parallel \ll k_B T_N \ll t_\perp$ where $t_\parallel\,(t_\perp)$ is the inter (intra) plane hopping integral and T_N is the three-dimensional Néel temperature. This regime is unusual because even though one is dealing with an itinerant fermion system, the inequality $t_\parallel \ll k_B T_N$ means that the smallest fermionic Matsubara frequency is larger than the dispersion in the parallel direction, making the three-dimensional band structure irrelevant for one-particle properties. In the language of Refs. [10] [11], there is "no coherent band motion" in the parallel direction. Physically, the extent of the thermal de Broglie wave packet in the direction perpendicular to the planes is smaller than the distance between planes, a situation that does not occur in a usual Fermi liquid since in the isotropic case the inequality $k_B T \ll E_F$ implies that the thermal de Broglie wavelength is much larger than the lattice spacing. Another way of describing this $t_\parallel \ll k_B T_N \ll t_\perp$ situation is to say that the itinerant electrons become unstable at the two-particle level while their motion in the third direction is still quasi-classical, or quantum incoherent, at the single-particle level because of thermal fluctuations. In the more usual situation, coherence at the one-particle level is established before the phase transition, namely $k_B T_N \ll t_\parallel \ll t_\perp$. These two regimes have been extensively discussed in the $d = 1$ to $d = 3$ crossover of Luttinger liquids by Bourbonnais and Caron [10] [11].

The above single-particle incoherent regime $t_\parallel \ll k_B T_N \ll t_\perp$ is likely to be the relevant one for high-temperature superconductors. While the parent insulating compound La_2CuO_4 has been extensively studied in the strong coupling limit, this type of compound is expected to be in an intermediate-coupling regime. Hence, it is legitimate to approach the problem not only from the strong-coupling limit [12] but also from the weak-coupling side, especially with the TPSC approach where all cutoffs are determined by the microscopic model. This problem is commented on at the end of the paper. More detailed quantitative comparisons with experiment will appear later.

II. TWO-PARTICLE SELF-CONSISTENT APPROACH

We start from the Hubbard model,

$$H = -\sum_{<ij>\sigma} t_{i,j}\left(c^\dagger_{i\sigma}c_{j\sigma} + c^\dagger_{j\sigma}c_{i\sigma}\right) + U\sum_i n_{i\uparrow}n_{i\downarrow}\ . \tag{1}$$

In this expression, the operator $c_{i\sigma}$ destroys an electron of spin σ at site i. Its adjoint $c^\dagger_{i\sigma}$ creates an electron. The symmetric hopping matrix $t_{i,j}$ determines the band structure. Double occupation of a site costs an energy U due to the screened Coulomb interaction. In the present section, the hopping parameters need not be specified. We work in units where $k_B = 1$, and $\hbar = 1$. As an example that occurs later, the dispersion relation in the d-dimensional nearest-neighbor model when the lattice spacing is a is given by

$$\epsilon_{\mathbf{k}} = -2t\sum_{i=1}^{d}(\cos k_i a)\,. \tag{2}$$

The nearest-neighbor quasi-two dimensional case will be another case of interest later,

$$\epsilon_{\mathbf{k}} = -2t_\perp\left(\cos k_x a_\perp + \cos k_y a_\perp\right) - 2t_\parallel \cos k_z a_\parallel. \tag{3}$$

The TPSC approach [7], [13] can be summarized as follows. One approximates spin and charge susceptibilities χ_{sp}, χ_{ch} by RPA-like forms but with two different effective interactions U_{sp} and U_{ch} which are then determined self-consistently. Although the susceptibilities have an RPA functional form, the physical properties of the theory are very different from RPA because of the self-consistency conditions on U_{sp} and U_{ch}. The necessity to have two different effective interactions for spin and for charge is dictated by the Pauli exclusion principle $\langle n_\sigma^2\rangle = \langle n_\sigma\rangle$ which implies that both χ_{sp} and χ_{ch} are related to only one local pair correlation function $\langle n_\uparrow n_\downarrow\rangle$. Indeed, using the fluctuation-dissipation theorem in Matsubara formalism we have the exact sum rules,

$$\langle n_\uparrow^2\rangle + \langle n_\downarrow^2\rangle + 2\langle n_\uparrow n_\downarrow\rangle - n^2 = \frac{1}{\beta N}\sum_{\widetilde{q}}\chi_{ch}(\widetilde{q}) \tag{4}$$

and

$$\langle n_\uparrow^2\rangle + \langle n_\downarrow^2\rangle - 2\langle n_\uparrow n_\downarrow\rangle = \frac{1}{\beta N}\sum_{\widetilde{q}} \chi_{sp}(\widetilde{q}) \tag{5}$$

where $\beta \equiv 1/T$, $n = \langle n_\uparrow\rangle + \langle n_\downarrow\rangle$, $\widetilde{q} = (\mathbf{q}, iq_n)$ with $\mathbf{q}$ the wave vectors of an N site lattice, and with $iq_n = 2\pi inT$ the bosonic Matsubara frequencies. The Pauli principle $\langle n_\sigma^2\rangle = \langle n_\sigma\rangle$ applied to the left-hand side of both equations with our RPA-like forms for χ_{sp}, χ_{ch} on the right-hand side lead to

$$n + 2\langle n_\uparrow n_\downarrow\rangle - n^2 = \frac{1}{\beta N}\sum_{\widetilde{q}} \frac{\chi_0(\widetilde{q})}{1+\frac{1}{2}U_{ch}\chi_0(\widetilde{q})}, \tag{6}$$

$$n - 2\langle n_\uparrow n_\downarrow\rangle = \frac{1}{\beta N}\sum_{\widetilde{q}} \frac{\chi_0(\widetilde{q})}{1-\frac{1}{2}U_{sp}\chi_0(\widetilde{q})}, \tag{7}$$

with $\chi_0(\widetilde{q})$ the susceptibility for non-interacting electrons.

If $\langle n_\uparrow n_\downarrow\rangle$ is known, U_{sp} and U_{ch} are determined from the above equations. This key quantity $\langle n_\uparrow n_\downarrow\rangle$ can be obtained from Monte Carlo simulations or by other means. However, it may be also be obtained self-consistently [7] by adding to the above set of equations the relation

$$U_{sp} = g_{\uparrow\downarrow}(0)\, U \quad ; \quad g_{\uparrow\downarrow}(0) \equiv \frac{\langle n_\uparrow n_\downarrow\rangle}{\langle n_\downarrow\rangle\langle n_\uparrow\rangle}. \tag{8}$$

Eqs.(7) and (8) define a set of self-consistent equations for U_{sp} that involve only two-particle quantities. We call this approach Two-Particle Self-Consistent to contrast it with other conserving approximations like Hartree-Fock or FLEX [14] that are self-consistent at the one-particle level, but not at the two-particle level. The above procedure [7] reproduces both Kanamori-Brueckner screening as well as the effect of Mermin-Wagner thermal fluctuations, giving a phase transition only at zero-temperature in two dimensions, as discussed in the following section. Quantitative agreement with Monte Carlo simulations on the nearest-neighbor [7] and next-nearest-neighbor models [8] is obtained [7] for all fillings and temperatures in the weak to intermediate coupling regime $U < 8t$.

We emphasize that deep in the critical regime, the *ansatz* Eq.(8) fails in the sense that $g_{\uparrow\downarrow}(0)$ eventually reaches zero at $T = 0$ in the nearest-neighbor Hubbard model at half-filling while there is no reason to believe that this really happens. The physically appropriate choice in the renormalized classical regime described below, is to keep the value of $g_{\uparrow\downarrow}(0)$ fixed at its crossover-temperature value. In the numerical calculations also described below, we are never far enough from T_X to have to worry about this. The value of $g_{\uparrow\downarrow}(0)$ is the one that is determined self-consistently.

III. CRITICAL BEHAVIOR OF THE TPSC APPROACH IN ARBITRARY DIMENSION

In this section we discuss the critical behavior of the TPSC approach in arbitrary dimension for hypercubic systems. It is convenient to set the lattice spacing to unity.

As one approaches a phase transition, one enters the *renormalized classical* regime, [1] where classical thermal fluctuations dominate. In this case, the universality class for *static* properties is fully determined by two exponents. Dynamics must also be considered so that one introduces a dynamical critical exponent.

We consider the case where the transition is at the antiferromagnetic wave vector $\mathbf{Q}_d$ in d dimensions: $\mathbf{Q}_2 = (\pi, \pi)$, $\mathbf{Q}_3 = (\pi, \pi, \pi)$ etc. Since $\mathbf{Q}_d$ is at the corner of the Brillouin zone, the spin susceptibility $\chi_0(\mathbf{Q}_d)$ is always, by symmetry, an extremum. This extremum is the absolute maximum at half-filling not only in the nearest-neighbor hopping model, but also in more general models with next-nearest-neighbor hopping [8] [15]. The nearest-neighbor model is discussed in more details at the end of this section. It has some special features resulting from the additional nesting symmetry. In the two-dimensional case, we also comment on peculiarities of nesting and on quantum-critical behavior [3] [2].

A. Renormalized classical regime.

As one decreases the temperature sufficiently close to the phase transition, there appears a small energy scale δU that measures the proximity to the phase transition as determined by the Stoner criterion. This scale is defined more

precisely in Eq.(13). The key physical point is that this energy scale is the smallest. In particular, it is smaller than the temperature

$$\delta U \ll T \tag{9}$$

so that the zero Matsubara frequency representing classical behavior dominates all others. The self-consistency conditions Eqs.(7)(8) then lead to a strong temperature dependence of δU. This is the renormalized-classical regime [1]. In this regime, the antiferromagnetic correlation length ξ becomes so large that [13]

$$\xi \gg \xi_{th} \tag{10}$$

where

$$\xi_{th} \equiv \frac{\langle v_F \rangle}{\pi T} \tag{11}$$

is the single-particle thermal de Broglie wavelength and $\langle v_F \rangle$ is the Fermi velocity averaged over the Fermi surface. This provides a partial justification for the usual procedure [5] [4] that eliminates completely the Fermionic variables and describes the system in terms of collective Bosonic variables, as is usually done in Hubbard-Stratonovich types of approaches. [5] [4]

We first show that when most of the temperature dependence of the susceptibility comes from the temperature dependence of δU, the RPA-like form that we have implies that *in any dimension* the dynamical exponent is $z = 2$ while the classical exponent $\gamma/\nu = 2 - \eta$ takes the value $\gamma/\nu = 2$. The other classical exponent ν is determined from the self-consistency condition Eq.(7). We show that the corresponding universality class is the same as the $n \to \infty$ limit of the $O(n)$ classical model. This universality class is known in turn to be the same as that of the spherical model. [16] We conclude this discussion with the lower critical dimension $d = 2$. There the exponent ν cannot strictly be defined since, as was shown before [7], the correlation length diverges exponentially at zero temperature instead of diverging as a power law at finite temperature. This behavior is also the one expected from the $n \to \infty$ model, although nesting leads to different temperature dependences that are explained further.

1. Exponents γ/ν and z in arbitrary dimension

The antiferromagnetic transition is characterized by the appearance of a small energy scale, or equivalently a large correlation length, in the retarded spin susceptibility

$$\chi^R_{sp}(\mathbf{q},\omega) = \frac{\chi^R_0(\mathbf{q},\omega)}{1 - \frac{1}{2} U_{sp} \chi^R_0(\mathbf{q},\omega)}. \tag{12}$$

The small energy scale is set by

$$\delta U = U_{mf,c} - U_{sp} \tag{13}$$

where the temperature-dependent "mean-field critical" interaction

$$U_{mf,c} \equiv 2/\chi_0(\mathbf{Q}_d, 0) \tag{14}$$

is the temperature-dependent value of U_{sp} at which a phase transition would occur according to mean-field theory. In the vicinity of this point the small energy scale δU allows us to approximate $\chi^R_{sp}(\mathbf{q},\omega)$ by expanding the denominator near $\mathbf{q} \approx \mathbf{Q}_d$ and $\omega \approx 0$ to obtain,

$$\chi^R_{sp}(\mathbf{q} + \mathbf{Q}_d,\omega) \approx \xi^2 \frac{2}{U_{sp} \xi_0^2} \left[\frac{1}{1 + \mathbf{q}^2 \xi^2 - i\omega \xi^2 / D} \right] \tag{15}$$

where the antiferromagnetic correlation length is defined by

$$\xi \equiv \xi_0 \left(\frac{U_{sp}}{\delta U} \right)^{1/2} \tag{16}$$

with the microscopic length scale set by

$$\xi_0^2 \equiv \frac{-1}{2\chi_0\left(\mathbf{Q}_d\right)} \left.\frac{\partial^2 \chi_0\left(\mathbf{q},0\right)}{\partial q_x^2}\right|_{\mathbf{q}=\mathbf{Q}_d}. \tag{17}$$

The microscopic diffusion constant D is defined on the other hand by

$$\frac{1}{D} \equiv \frac{\tau_0}{\xi_0^2} \tag{18}$$

where the microscopic relaxation time is,

$$\tau_0 = \frac{1}{\chi_0\left(\mathbf{Q}_d\right)} \left.\frac{\partial \chi_0^R\left(\mathbf{Q}_d,\omega\right)}{\partial i\omega}\right|_{\omega=0}. \tag{19}$$

This relaxation-time is non-zero in both models B and C where the Fermi surface intersects the magnetic Brillouin zone.

In the presence of a large correlation length ξ the scaling $q \sim \xi^{-1}$ and $\omega \sim \xi^{-2}$ justifies the neglect of higher-order terms in the expansion Eq.(15). Comparing the approximate form Eq.(15) with the general scaling expression

$$\chi_{sp}^R(\mathbf{q}+\mathbf{Q}_d,\omega) \approx \xi^{\gamma/\nu} X\left(\mathbf{q}\xi, \omega\xi^z\right) \tag{20}$$

where $X\left(\mathbf{q}\xi, \omega\xi^z\right)$ is a scaling function, we immediately have the announced results,

$$\frac{\gamma}{\nu} = 2 \quad ; \quad z = 2. \tag{21}$$

The Fisher scaling law $\eta = 2 - \frac{\gamma}{\nu}$ shows that the anomalous exponent η vanishes as in mean-field theory. In the following paragraphs, we compute the remaining exponent ν to show that above four dimensions we do recover mean-field theory $\nu = 1/2$ while for $2 < d < 4$, we have the $n \to \infty$ result $\nu = 1/\left(d-2\right)$.

2. Exponent ν in $2 < d < 4$ and equivalence to spherical ($n \to \infty$) model.

The correlation length exponent is determined by solving self-consistently Eqs.(7) and (8) for the quantity $\langle n_\uparrow n_\downarrow \rangle = U_{sp}/U$. In general, we do this numerically using some technical tricks that are discussed below. With this procedure, no arbitrariness is left in the cutoffs, that are entirely determined from the microscopic Hubbard model. However, to study analytically the critical behavior, we notice that there is a crossover temperature T_X below which the presence of the small energy scale $\delta U << T$ makes the zero Matsubara frequency component in the sum rule Eq.(7) much larger than all the others. This is the *renormalized classical regime* discussed above. Its existence is a manifestation of critical-slowing down, $\omega \sim \xi^{-2} \sim \delta U$ near a phase transition. Using the approximate Lorentzian form Eq.(15) for the $i\omega = iq_n = 0$ component we rewrite Eq.(7) as follows, after a trivial shift of integration variables,

$$\tilde{\sigma}^2 = \frac{2T}{U_{sp}\xi_0^2} \int \frac{d^d q}{(2\pi)^d} \frac{\xi^2}{1+q^2\xi^2}. \tag{22}$$

In this equation,

$$\tilde{\sigma}^2 = n - 2\langle n_\uparrow n_\downarrow \rangle - C \leq 1 \tag{23}$$

is the local moment $n - 2\langle n_\uparrow n_\downarrow \rangle$ minus corrections C that come from the sum over non-zero Matsubara frequencies (quantum effects) and from the terms neglected in the Lorentzian approximation, namely those coming from short distances $\left(\mathbf{q}-\mathbf{Q}\right)^2 \gg \xi^{-2}$.

Contrary to the strong-coupling case, and contrary to more usual approaches [2], $\tilde{\sigma}^2$ *here is temperature dependent* because both $\langle n_\uparrow n_\downarrow \rangle$ and C are. Nevertheless, to find the critical behavior analytically, it suffices to notice that this dependence is regular. In fact, we have that when $T \simeq T_X$, the double occupancy can be approximated by $\langle n_\uparrow n_\downarrow \rangle = U_{sp}/U \approx U_{mf,c}/U$ when $\delta U \to 0$.

At the Néel temperature, T_N, the correlation length diverges, $\xi = \infty$, so that Eq.(22) determines the Néel temperature through

$$\tilde{\sigma}^2 = \frac{2T_N}{U_{sp}\xi_0^2} \int \frac{d^d q}{(2\pi)^d} \frac{1}{q^2}. \tag{24}$$

The wave vector integration is cutoff at large q by the Brillouin zone ($-\pi < q_i < \pi$ for any component q_i) so that the only divergence occurs from $q = 0$ in $d \leq 2$ ($q = 0 \rightarrow q = \mathbf{Q}_d$ in the original integration variables). Since the left-hand side of this Eq.(24) is finite, this divergence prevents the existence of a finite-temperature antiferromagnetic phase transition in two dimensions or less.

To find the correlation length exponent in $2 < d < 4$, one rewrites Eq.(22) in the form,

$$\tilde{\sigma}^2 = \frac{2T}{U_{sp}\xi_0^2} \int \frac{d^d q}{(2\pi)^d} \left[\frac{\xi^2}{1+q^2\xi^2} - \frac{1}{q^2} \right] + \frac{2T}{U_{sp}\xi_0^2} \int \frac{d^d q}{(2\pi)^d} \left[\frac{1}{q^2} \right]. \tag{25}$$

Using the expression for the Néel temperature Eq.(24), this last expression becomes,

$$\tilde{\sigma}^2 \left(1 - \frac{T}{T_N} \right) = \frac{2T}{U_{sp}\xi_0^2} \xi^{2-d} \int \frac{d^d (q\xi)}{(2\pi)^d} \left[\frac{1}{1+q^2\xi^2} - \frac{1}{q^2\xi^2} \right]. \tag{26}$$

Since the integral converges at $q\xi \rightarrow \infty$ for $2 < d < 4$, it can be replaced by a ξ-independent negative number and one finds,

$$\xi \sim \left(\frac{T}{T_N} - 1 \right)^{1/(2-d)} \sim \left(\frac{T}{T_N} - 1 \right)^{-\nu} \tag{27}$$

which gives,

$$\nu = \frac{1}{d-2}. \tag{28}$$

This exponent and $\gamma/\nu = 2$, found in the previous section, are the same as the one for the Berlin-Kac spherical model [16] or equivalently for the generalized Heisenberg model where spins are n components vectors and $n \rightarrow \infty$. In three dimensions, this leads to

$$\nu = 1, \quad \gamma = 2, \quad \alpha = -1, \quad \beta = \frac{1}{2}, \quad \eta = 0 \text{ and } \delta = 5. \tag{29}$$

For comparison, numerical results [17] for the $3D$ Heisenberg ($n = 3$) model give $\nu \sim 0.7$ and $\gamma \sim 1.4$.

Above $d = 4$, one recovers the mean-field results $\gamma = 2\nu$ and $\nu = 1/2$. This last result follows from the fact that in $d > 4$, the integral in Eq.(26) is dominated by the large momentum cutoff so that for $\xi >> 1$, $\left(1 - \frac{T}{T_N}\right) \sim \xi^{-2} \int d^d q/q^4$.

3. Two-dimensional case

We have already proven in the last subsection that the transition temperature vanishes in two dimensions. The correlation length may be found [7] in the renormalized classical regime directly by performing the integral Eq.(22) in $d = 2$,

$$\xi = \xi_0 \left(U_{sp}/\delta U \right)^{\frac{1}{2}} \sim \Lambda^{-1} \exp(\pi \tilde{\sigma}^2 \xi_0^2 U_{sp}/T) \tag{30}$$

where $\Lambda \sim \pi$ is usually of the order of the size of the Brillouin zone, but not always as we discuss below.

In $d = 2$, we call T_X the temperature at which δU is much smaller than temperature and the magnetic correlation length ξ grows exponentially. While in higher dimensions a phase transition occurs at finite temperature, in $d = 2$ the critical regime with an exponentially increasing ξ extends all the way to zero temperature. For example, the temperature T_X is plotted as a function of filling in the two-dimensional nearest-neighbor Hubbard model for $U = 2.5$ in Fig.1 of Ref. [7]. In this reference, T_X is called a quasi-critical temperature. We stress that there is a range of fillings near half-filling where at T_X it is the antiferromagnetic wave vector that grows, despite the fact that at zero-temperature the phase transition would be at an incommensurate wave vector.

The exponential growth of the two-dimensional ξ clearly suggests that small $3D$ effects existing in real systems may stabilize long-range order at $\mathbf{Q}_{d=3}$, before $T = 0$. We later characterize the crossover driven by a small $3D$ hopping parameter $t_\parallel \ll t_\perp$ from two-dimensional critical behavior to three-dimensional critical behavior. But before, we comment on the two-dimensional quantum-critical regime and on peculiarities induced by nesting in the renormalized-classical regime.

B. Quantum-critical regime

When there is a critical value of the interaction U_c *at zero temperature* where one finds a paramagnet for $U < U_c$ and an antiferromagnet for $U > U_c$, then the $T = 0$, $U = U_c$ point of the phase diagram is a quantum critical point. [4] The vicinity of this point in two dimensions has been studied again recently [2]. In order to study such a regime within the Hubbard model at half-filling, one must introduce next-nearest-neighbor hopping since $U_c\,(T = 0) = 0$ at this filling in the nearest-neighbor model. One finds that the TPSC approach has precisely the $n \to \infty$ model A or model B quantum critical behavior [2], depending on the specific microscopic model. In particular, ξ scales as $1/T$ as one approaches the two-dimensional quantum critical point from finite temperature. Again, in the TPSC approach the cutoffs are specified without ambiguity. Model C, the perfect nesting case, is relevant only to the renormalized-classical case, as we now discuss.

C. Peculiarities induced by perfect nesting in the renormalized-classical regime, especially in $d = 2$.

The dispersion relation of the nearest-neighbor Hubbard model on hypercubic lattices in arbitrary dimension satisfies $\epsilon_{\mathbf{k}+\mathbf{Q}_d} = -\epsilon_{\mathbf{k}}$. Furthermore, at half-filling the particle-hole symmetry implies that the Fermi surface is fully nested, namely $\mu = 0$ so that the equality $\epsilon_{\mathbf{k}+\mathbf{Q}_d} - \mu = -(\epsilon_{\mathbf{k}} - \mu)$ is satisfied for all wave vectors $\mathbf{k}$. Slightly away from half-filling, nesting in the form $\epsilon_{\mathbf{k}+\mathbf{Q}_d} - \mu \sim -(\epsilon_{\mathbf{k}} - \mu)$ is also a good *approximation* at finite temperature as long as $T > \mu$, as discussed above. When there is perfect nesting, the zero-temperature critical interaction vanishes ($U_c = 0$). Hence the fully nested Fermi surface, referred to as Model C above, does not have the simple quantum-critical point described in the previous sub-section.

When there is perfect nesting, the microscopic interaction-independent quantities ξ_0^2 and τ_0 have a peculiar temperature dependence. This occurs because they are derivatives of the susceptibility which itself contains logarithmic singularities in the zero-temperature limit. These quantities are evaluated in two dimensions and in the quasi two-dimensional case in Appendix A. Dimensional arguments that follow simply from this appendix show that in $d > 2$

$$\xi_0^2 \sim 1/\left(T^2 \ln T^{-1}\right) \tag{31}$$

$$\tau_0 \sim 1/\left(T \ln T^{-1}\right). \tag{32}$$

In $d = 2$, the $\ln T^{-1}$ is replaced by $\ln^2 T^{-1}$. [18]

By contrast, in the case of second-neighbor hopping, nesting is lost and the above quantities are temperature independent for a wide range of values of the second-neighbor hopping constant. The above temperature dependencies are then a special property of nesting. In $d > 2$ however, the above temperature dependencies are completely negligible in the critical regime since near the phase transition one can replace T in the above expressions by T_N.

The only issue then is in two dimensions where the phase transition occurs at zero temperature. Even neglecting logarithms for the moment, one sees that since ξ_0^2 scales as $1/T^2$ over a wide temperature range the correlation length in Eq.(30) scales as $\exp\left(cst/T^3\right)$. By contrast, in strong coupling, or in the non-nesting case of the weak-coupling limit, the correlation length scales as $\exp(cst/T)$.

The $\exp\left(cst/\left(T^3 \ln^2 T^{-1}\right)\right)$ behavior is however largely an unsolved problem. Indeed, in the critical regime in two dimensions, fluctuations remove the quasiparticle peak and replace it by precursors of the antiferromagnetic bands, as shown in Ref. [13]. It is possible then that, in this regime, a more self-consistent treatment would lead to ξ_0^2 independent of temperature, as in the strong coupling case or the non-nested weak-coupling case. It is also likely that there will be an intermediate temperature range where the $\exp\left(cst/\left(T^3 \ln^2 T^{-1}\right)\right)$ regime prevails, even if deep in the critical regime self-consistency leads to $\exp\left(cst/T\right)$ behavior.

It is important to recall that in practical calculations in the TPSC approach, one obtains a numerical value for the correlation length without adjustable parameter. For example in Fig.1 we present the temperature dependence of the correlation length for the two-dimensional nearest-neighbor Hubbard model. As discussed in Appendix A, in this case

$$\xi_0^2 \simeq 0.021 U_{mf,c} t_\perp^2 a_\perp^2 / T^2 \tag{33}$$

and $U_{sp} \simeq U_{mf,c}$ so that from the slope of the plot and from Eq.(30) one finds $\tilde{\sigma}^2 \simeq 0.21$. From the plot we can also extract $\Lambda^{-1} \simeq 0.022$ so that ξ is known without adjustable parameter. Appendix B explains physically the orders of magnitude taken by $\tilde{\sigma}^2$ and Λ^{-1} in this model. Similar calculations can be done for arbitrary band structure. In strong-coupling calculations, [1] [3] one obtains $\xi \sim \Lambda^{-1} \exp(2\pi\rho_S/T)$ with ρ_S a cutoff-dependent quantity that can be evaluated only with Monte Carlo simulations.

Another consequence of the temperature behavior of ξ_0 in Eq.(31) is that *above* T_X there is a range of temperatures for which the antiferromagnetic correlation length scales as $\xi \sim \xi_0 \sim 1/T$. This behavior should not be confused with quantum-critical behavior, even though the power-law scaling of the correlation length is the same. Indeed, one finds that the argument of the exponential in Eq.(30) is larger than unity in the corresponding regime while in the quantum-critical regime the argument of the exponential should be much less than unity. [2] In fact the temperature dependence of the staggered susceptibility for $T > T_X$ is also-different from the quantum critical result.

IV. QUASI TWO-DIMENSIONAL SYSTEMS: RENORMALIZED CLASSICAL CROSSOVER FROM $D = 2$ TO $D = 3$.

The general discussion of universality in the renormalized-classical crossover from $d = 2$ to $d = 3$ appears in Appendices C and D. In the present section, we first clarify the various regimes of crossover, according to whether or not single-particle coherence in the third dimension is established before the phase transition. Then, we go on to discuss the case $t_\parallel \ll T_N < T_X$ where the SDW instability occurs before interplane single-particle coherence is established. More specifically, we find the scaling of the Néel temperature with $t_\perp/t_\parallel$ as well as the size of the three-dimensional critical regime with the corresponding exponents, showing that the results are those of the $n \to \infty$ limit. We restore the lattice spacing units $a_\parallel$ along the three-dimensional axis and $a_\perp$ in the planes. We assume however that the ratio $a_\parallel/a_\perp$ is usually of order unity and numerical calculations are done for $a_\parallel/a_\perp = 1$

A. One-particle and two-particle crossover from $d = 2$ to $d = 3$.

We consider in this section the highly anisotropic situation where hopping between planes $t_\parallel$ is much smaller than in-plane hopping, $t_\perp$,

$$t_\parallel \ll t_\perp \tag{34}$$

as might occur in the high-temperature superconductor parent compound La_2CuO_4. In this case, we have that the three-dimensional transition temperature to long-range order T_N is always less than the crossover temperature T_X to the characteristic exponential behavior of the correlation length in two dimensions

$$T_N < T_X. \tag{35}$$

This is so because the microscopic in-plane $\xi_0^\perp$ and out of plane $\xi_0^\parallel$ lengths satisfy $\xi_0^\perp \gg \xi_0^\parallel$.

The crossover temperature to two-dimensional behavior for itinerant antiferromagnet always satisfies

$$T_X < t_\perp. \tag{36}$$

Two limiting cases are then possible, depending on interaction and on hopping parallel to the three-dimensional axis $t_\parallel$:

a) Weak coupling or small anisotropy limit:

$$T_N < T_X \ll t_\parallel. \tag{37}$$

In this case, when the transition to three-dimensional behavior occurs the three-dimensional Fermi surface is relevant since the thermal de Broglie wavelength $v_F^\parallel/(\pi T) \sim t_\parallel a_\parallel/T$ is larger than the distance between planes. In other words, the three-dimensional band structure is relevant to the behavior of *single-particle* propagators in Matsubara frequencies before the phase transition occurs. Fermions are quantum-mechanically coherent over more than a single plane and nesting generally plays a role in the value of the ordering wave vector. The crossover from two to three dimensional *critical* behavior would occur in a manner analogous to the anisotropic Heisenberg model [19] [20] [21] [22].

b) Intermediate coupling or very large anisotropy:

$$t_\parallel \ll T_N < T_X. \tag{38}$$

Here, long-range order is established before the single-particle coherence occurs between planes. A phase transition occurs only because of *two-particle* (or particle-hole) coherent hopping. When the phase transition occurs, thermal fluctuations are still large enough that coherent single-particle band motion in the parallel direction has not occured

yet. There are several ways of explaining physically what this last statement means. For example, it is clear that when $t_\parallel \ll T$, features of the band structure in the parallel direction are irrelevant for single-particle properties since the first Matsubara frequency is larger than the bandwidth in that direction. The motion *between* planes is still in that sense quasi-classical when the phase transition occurs. Another way of saying what this means is that the thermally induced uncertainty in the parallel wave vector is equal to the extent of the Brillouin zone in that direction, corresponding, via the uncertainty principle, to a confinement within each plane.

We do not discuss the intermediate case $T_N < t_\parallel < T_X$ but concentrate instead on the very large anisotropy - intermediate coupling limit just introduced.

B. Numerical solutions

The scaling behavior of the Néel temperature T_N and of the three-dimensional crossover temperature are derived in the following two sections. We first present the numerical results obtained from the solution of the self-consistency relations Eqs.(7) and (8). The numerical integration in Eq.(7) is made possible by rewriting this equation in the form,

$$n - 2\langle n_\uparrow n_\downarrow \rangle = T a_\parallel a_\perp^2 \int \frac{d^3q}{(2\pi)^3} \sum_{iq_n} \left[\chi_{sp}\left(\mathbf{q}, iq_n\right) - \chi_{sp}^{as}\left(\mathbf{q},0\right) \delta_{n,0} \right] + T a_\parallel a_\perp^2 \int \frac{d^3q}{(2\pi)^3} \chi_{sp}^{as}\left(\mathbf{q},0\right). \tag{39}$$

The sum over large Matsubara frequencies can be approximated by an integral in a controlled manner. The subtraction in the first integral removes singularities of the integrand and makes the integral well behaved. Since the transition occurs in the single-particle incoherent regime Eq.(38), the integrand in square brackets is independent of $q_\parallel$ above the Néel temperature. All quantities involving $t_\parallel$ come from the second integral over the asymptotic expression for the susceptibility

$$\chi_{sp}^{as}\left(\mathbf{q}+\mathbf{Q}_3,0\right) \equiv \frac{2}{\delta U} \frac{1}{1+\xi_\parallel^2 q_\parallel^2 + \xi_\perp^2 q_\perp^2} \tag{40}$$

where

$$\xi_\perp \equiv \xi_0^\perp (U_{sp}/\delta U)^{1/2}, \tag{41}$$

$$\xi_\parallel \equiv \xi_0^\parallel (U_{sp}/\delta U)^{1/2}. \tag{42}$$

To have sufficient precision for large two-dimensional correlation lengths, it is important to evaluate analytically $\xi_0^\perp$, $\xi_0^\parallel$, as well as the integral of Eq.(40) appearing in the consistency equation Eq.(39). This is done respectively in Appendices A and C. To perform the second derivatives in the definition of $\xi_0^\perp$, $\xi_0^\parallel$, we expand $\chi_0(\mathbf{Q}_3)$ in powers of $t_\parallel/T$, keeping only the first non-zero term: thus $\xi_0^\perp$ does not differ from the one already presented in Eq. (33). It is shown in Appendix A that over a wide range of temperatures we have

$$\frac{\partial^2 \chi_0\left(\mathbf{Q}_3\right)}{\partial q_\perp^2} \sim a_\perp^2 \left[\frac{t_\perp^2}{T^2} + O(t_\parallel/T) \right], \tag{43}$$

and

$$\frac{\partial^2 \chi_0\left(\mathbf{Q}_3\right)}{\partial q_\parallel^2} \sim a_\parallel^2 \left[\frac{t_\parallel^2}{T^2} + O(t_\parallel^3/T^3) \right]. \tag{44}$$

The inter-plane hopping $t_\parallel$ in Eqs.(39) and (40) occurs explicitly only in $\xi_0^\parallel$ and the above results imply that,

$$\frac{\xi_0^\parallel}{\xi_0^\perp} \sim \frac{\xi_\parallel}{\xi_\perp} \sim \frac{t_\parallel a_\parallel}{t_\perp a_\perp}. \tag{45}$$

We present numerical results for the nearest-neighbor Hubbard model in units where $a_\parallel = a_\perp = 1$ and $t_\perp = 1$. The value of $T_N\left(t_\parallel\right)$ appears in Figs.2 and 3 for $U = 4$. In Fig.2, we clearly see that T_N becomes almost equal to $T_X \approx 0.2$ for $t_\parallel$ still quite small. The scaling of $T_N\left(t_\parallel\right)$ shown in Fig.3 is explained in the following subsection. Fig.4

shows the variation of the in-plane correlation length $\xi_\perp$ as a function of temperature for various $t_\parallel$, again for $U = 4$. For the purely two-dimensional case $t_\parallel = 0$, one can observe for $T \leq T_X \simeq 0.2$ the exponential behavior mentioned in the preceding section. At a temperature about 0.16, the in-plane correlation length $\xi_\perp$ is already as much as 10^3 (in units where lattice space is unity). For $10^{-3} \leq t_\parallel \leq 10^{-1}$, $\xi_\perp$ diverges at the Néel temperature located in the narrow range $0.16 \leq T_N \leq 0.2$. For $t_\parallel \neq 0$, it is also clear that the crossover to three-dimensional behavior occurs in an extremely narrow temperature range. This is explained below. Note that the last few curves on the right-hand side are at the limit of validity of our approximations.

We note that for $U = 4t$, we find that at $T = T_N$ the local moment is equal to three quarters of the full moment in the atomic limit, *i.e.* $n - 2\langle n_\uparrow\rangle\langle n_\downarrow\rangle g_{\uparrow\downarrow}(0) = 0.75$, $g_{\uparrow\downarrow}(0) = \langle n_\uparrow n_\downarrow\rangle/\langle n_\uparrow\rangle\langle n_\downarrow\rangle$. This number is only weakly dependent on temperature in the range studied.

C. Dependence of the Néel temperature T_N on $t_\parallel$. Crossover exponent.

From the discussion of the previous section, Eqs.(39)(40)(22) we know that the singular part of the self-consistency condition may be written in the following form in the quasi-two dimensional case,

$$\tilde{\sigma}^2 = \frac{2Ta_\parallel a_\perp^2}{U_{sp}\left(\xi_0^\perp\right)^2}\int\frac{d^3q}{(2\pi)^3}\frac{1}{q_\perp^2 + \xi_\perp^{-2} + \left(\frac{\xi^\parallel}{\xi^\perp}\right)^2 q_\parallel^2}. \tag{46}$$

The integral can be done exactly, as in Appendix C, and all the results obtained in this subsection and the following one can be obtained from limiting cases of this general analytical result, as shown in Appendix D. Here we make approximations directly on the integrals since this makes the Physics of the results more transparent. Although arbitrary cutoffs appear in the analytical expressions, we re-emphasize that in the numerical calculations of the previous section the cutoffs are simply given by the Brillouin zone and there is no arbitrary scale in the results.

At T_N, we have $\xi_\perp^{-2} = 0$. Furthermore, from Eqs.(41) and (42) we find $\xi_\parallel/\xi_\perp = \xi_0^\parallel/\xi_0^\perp$ so that the above integral Eq.(46) takes the form

$$\tilde{\sigma}^2 = \frac{2T_N a_\parallel a_\perp^2}{U_{sp}\left(\xi_0^\perp\right)^2}\int\frac{d^2q_\perp}{(2\pi)^2}\left[\int\frac{dq_\parallel}{2\pi}\frac{1}{q_\perp^2 + \left(\frac{\xi_0^\parallel}{\xi_0^\perp}\right)^2 q_\parallel^2}\right]. \tag{47}$$

Using the mean-value theorem for the integral over $q_\parallel$ we have

$$\tilde{\sigma}^2 = \frac{2T_N a_\perp^2}{U_{sp}\left(\xi_0^\perp\right)^2}\int\frac{d^2q_\perp}{(2\pi)^2}\left[\frac{1}{q_\perp^2 + \left(\frac{\xi_0^\parallel}{\xi_0^\perp}\right)^2\widetilde{\Lambda}^2}\right] \tag{48}$$

where $\widetilde{\Lambda}$ is a constant that we need not specify. It is contained in the range $0 < \left|\widetilde{\Lambda}\right| < \pi/a_\parallel$. The above integral is the same as the one that determines the correlation length in two dimensions Eq.(22), hence at T_N we have that

$$\xi_\perp^{-2}(T_N) = \left(\frac{\xi_0^\parallel}{\xi_0^\perp}\right)^2\widetilde{\Lambda}^2 \propto \left(\frac{t_\parallel a_\parallel}{t_\perp a_\perp}\right)^2\widetilde{\Lambda}^2. \tag{49}$$

Comparing with the general theory of Appendix D where it is argued that $\xi_\perp^{-\phi/\nu}(T_N) \sim t_\parallel^2$, we see that $\phi/\nu = 2$. In other words, $\phi/\nu = \gamma/\nu = 2$ and the crossover exponent [17] ϕ is here equal to γ as is usually the case in the $n \to \infty$ model. [23] We obtain, using the expression (30) for the correlation length in two dimensions,

$$\frac{1}{T_N} = \frac{a_\perp^2}{\pi\widetilde{\sigma}^2 U_{sp}\left(\xi_0^\perp\right)^2}\left[\ln\frac{t_\perp}{t_\parallel} + c\right] \tag{50}$$

where c is a non-universal constant of order unity.

In the special case of perfect nesting (half-filled nearest-neighbor hopping model), the microscopic length $\xi_0^{\perp}$ is temperature dependent, as shown in Appendix A

$$\left(\xi_0^{\perp}\right)^2 \sim a_{\perp}^2 \frac{0.085}{T^2} \frac{1}{2\chi\left(\mathbf{Q}_2\right)}. \tag{51}$$

Using this result as well as $U_{mf,c} \equiv 2/\chi\left(\mathbf{Q}_2\right) \approx U_{sp}$ at $T_X \approx T_N$ gives the scaling illustrated in Fig.3 for the case $a_{\perp}/a_{\parallel} = 1$ namely

$$\frac{1}{T_N} \sim \frac{T_N^2}{U_{mf,c}^2} \left|\ln \frac{t_{\parallel}}{t_{\perp}}\right| \tag{52}$$

The logarithmic behavior in Eq.(50) is typical of systems that undergo a dimensional crossover from their lower critical dimension. For example, the analog of Eq.(49) in the anisotropic Heisenberg case would read, [19]

$$\xi_{\perp}^{-2}\left(T_N\right) \sim \left(\frac{J_{\parallel}}{J_{\perp}}\right) \widetilde{\Lambda}^2 \tag{53}$$

leading to [19] $T_N^{-1} \sim \ln\left(\frac{J_{\parallel}}{J_{\perp}}\right)$. The above results Eqs.(49) and (53) are suggested by the simple RPA-like form $\chi_{3d} \sim \chi_{2d}/\left(1 - J_{\parallel}\chi_{2d}\right)$ with $J_{\parallel}\chi_{2d} \sim 1$ at the transition and $\chi_{2d} \sim \xi_{\perp}^{\gamma/\nu} \sim \xi_{\perp}^2 \sim \exp\left(J_{\perp} cst/T\right)$. As in the previous section, the quantity $U_{sp}\left(\xi_0^{\perp,\parallel}\right)^2$ plays a role analogous to the exchange constants $J_{\perp\parallel,}$. In the perfect nesting case, these effective exchange constants would be temperature dependent since $U_{sp}\left(\xi_0^{\perp,\parallel}\right)^2 \sim U_{sp}\left(t_{\perp,\parallel}\right)^2/T^2$. Note that in the crossover from one-dimensional Luttinger liquid behavior to three-dimensional long-range order, the effective exchange constant $J_{\perp}$ also scales [10] [11] as $ut_{\perp}^2/T^2$, with u a running coupling constant. The one-dimensional Fermi surface is always nested.

D. Size of the three-dimensional critical region.

The singular temperature dependence of the correlation length is obtained from the equation

$$\tilde{\sigma}^2 = \frac{2Ta_{\parallel}a_{\perp}^2}{\delta U} \int \frac{d^3q}{(2\pi)^3} \frac{1}{1 + \xi_{\perp}^2 q_{\perp}^2 + \xi_{\parallel}^2 q_{\parallel}^2}. \tag{54}$$

Since the ratio $\xi_{\parallel}/\xi_{\perp} = \xi_0^{\parallel}/\xi_0^{\perp}$ is temperature independent, a simple change of integration variables shows that near T_N the scaling of both correlation lengths with temperature is identical to the isotropic three-dimensional case. In other words, the critical behavior near the phase transition is that of the three-dimensional system. However, as one increases the temperature away from T_N, the correlation lengths can decrease until $\xi_{\parallel} \ll a_{\parallel}$ while at the same time $\xi_{\perp} \gg a_{\perp}$. When $\xi_{\parallel} \ll a_{\parallel}$, the integral Eq.(54) is essentially two-dimensional and for $\xi_{\perp} \gg a_{\perp}$ one should observe the characteristic exponential temperature dependence of the two-dimensional correlation length.

As usual the definition of crossover contains some arbitrariness, so let us choose

$$\xi_{\parallel}\left(T^*\right) = a_{\parallel} \tag{55}$$

as the definition of the crossover temperature T^* between $d = 2$ and $d = 3$ critical behavior. In that regime, the correlation length Eq.(55) scales with temperature as in the $d = 2$ regime Eq.(30) except that, as argued before, $\xi_{\parallel}$ is smaller by a factor $\left(\xi_0^{\parallel}/\xi_0^{\perp}\right) = \left(t_{\parallel}a_{\parallel}\right)/\left(t_{\perp}a_{\perp}\right)$, hence we obtain for T^*

$$\frac{1}{T^*} = \frac{a_{\perp}^2}{\pi\tilde{\sigma}^2 U_{sp}\left(\xi_0^{\perp}\right)^2} \left[\ln\left(\frac{t_{\perp}}{t_{\parallel}}\right) + c'\right] \tag{56}$$

where c' is a non-universal constant of order unity. The size of the crossover region is thus

$$1 - \frac{T_N}{T^*} = T_N \frac{a_{\perp}^2}{\pi\tilde{\sigma}^2 U_{sp}\left(\xi_0^{\perp}\right)^2}\left(c - c'\right) = \frac{\left(c - c'\right)}{\ln\left(\frac{t_{\perp}}{t_{\parallel}}\right) + c} \sim \frac{1}{\ln\left(\frac{t_{\perp}}{t_{\parallel}}\right)}. \tag{57}$$

The above results Eqs.(55) to (57) are as expected from the usual theory of critical phenomena exposed in Appendix D. In particular, the scaling of T^* with $t_\parallel/t_\perp$ is the same as that of T_N. The smallness of the crossover region from $d=2$ to $d=3$ critical behavior in Fig.4 follows from the above considerations. The smaller is T_N, the smaller is T^*. The above situation should be contrasted with the problem of crossover from $d=3$ to $d=2$ in Helium films, studied by Fisher and Barber [24] many years ago. In that case, power law scaling occurred everywhere, giving quite different expressions for the scaling of T^* and T_N.

Given $\xi_\parallel(T^*)=\xi_0^\parallel(T^*)\left(U_{sp}/\delta U(T^*)\right)^{1/2}$, and $\xi_0^\parallel \sim t_\parallel$, the above relation $\xi_\parallel(T^*)=a_\parallel$ means that $\delta U(T^*)$ should scale as $t_\parallel^2$. Similarly we should have $\delta U(T_N)\sim t_\parallel^2$. We checked numerically [25] that the scaling with $t_\parallel$ holds for $t_\parallel<0.05$ in the half-filled nearest-neighbor model with $U=4t_\perp$.

V. CONCLUSION

We have shown that the TPSC approach allows one to study all aspects of nearly antiferromagnetic itinerant electrons in one-band Hubbard models. The method is in quantitative agreement with Monte Carlo simulations in the non-critical regime [7] [8] while in the critical regime, (renormalized classical or quantum critical) the relatively weak temperature dependence of the local moment leads to the same critical behavior as strong-coupling models to leading order in the $1/n$ expansion, namely in the $n\to\infty$ limit. There is no arbitrary cutoff so that all results can be obtained as a function of lattice spacing, hopping integral and interaction parameter. Fermi surface effects are apparent, in particular in the case of perfect nesting where the two-dimensional renormalized-classical correlation length diverges as $\exp\left(cst/\left(T^3\ln^2 T\right)\right)$ instead of $\exp(cst/T)$.

We have applied the method to a detailed study of the renormalized-classical crossover from two to three dimensions where we have highlighted the existence of a regime where the three-dimensional Néel instability occurs before thermal fluctuations become small enough to allow coherent single-particle band motion between planes. An analogous phenomenon occurs in quasi-one dimensional systems [10] [11]. The TPSC approach can be applied to study realistic cases. For La_2CuO_4 we will show in a subsequent publication that with second-neighbor hopping one can fit experiments on the magnetic structure factor.

The generalization of the TPSC approach beyond leading order in $1/n$ is left open. Also, the effect of self-energy feedback [13] on $\exp\left(cst/\left(T^3\ln^2 T\right)\right)$ behavior of the correlation length in the two-dimensional nesting case should be cleared in further studies. Finally, the universal $d=2$ to $d=3$ crossover discussed in Appendix D should be investigated beyond leading order in $1/n$.

We are indebted to C. Bourbonnais for numerous discussions and key ideas. We also thank David Sénéchal for discussions and D.S. Fisher for pointing out Ref. [22]. We acknowledge the support of the Natural Sciences and Engineering Research Council of Canada (NSERC), the Fonds pour la formation de chercheurs et l'aide à la recherche from the Government of Québec (FCAR) and (A.-M.S.T.) the Canadian Institute for Advanced Research (CIAR) and the Killam foundation.

APPENDIX A: $\xi_0^{\parallel,\perp}$ AND τ_0 IN THE CASE OF NESTING

In this appendix we derive expressions for the out of plane $\xi_0^\parallel$ and in-plane $\xi_0^\perp$ microscopic lengths,

$$\xi_0^{\parallel,\perp}=\frac{-1}{2\chi_0(\mathbf{Q}_d)}\left.\frac{\partial^2\chi_0(\mathbf{q},0)}{\partial q_{\parallel,\perp}^2}\right|_{\mathbf{q}=\mathbf{Q}_d} \tag{A1}$$

as well as for the microscopic relaxation time τ_0 in Eq.(19)

$$\tau_0=\frac{1}{\chi_0(\mathbf{Q}_d)}\left.\frac{\partial\chi_0^R(\mathbf{Q}_d,\omega)}{\partial i\omega}\right|_{\omega=0} \tag{A2}$$

for the quasi two-dimensional antiferromagnet $\mathbf{Q}_3=(\pi,\pi,\pi)$, in the regime $t_\parallel\ll T_N<T_X$ of Eq.(38). We also assume that $\mu\ll T$ so that the maximum of the static susceptibility is at $\mathbf{Q}_3$ even away from half-filling.

We start from the retarded Lindhard function in d dimensions

$$\chi_0^R(\mathbf{q},\omega)=2a_\parallel a_\perp^2\int_{BZ}\frac{d^dk}{(2\pi)^d}\,\frac{f(\epsilon_{\mathbf{k}+\mathbf{q}}-\mu)-f(\epsilon_{\mathbf{k}}-\mu)}{\omega+i\eta-\epsilon_{\mathbf{k}+\mathbf{q}}+\epsilon_{\mathbf{k}}}, \tag{A3}$$

where f is the Fermi function, μ the chemical potential ($\mu = 0$ at half-filling for our Hamiltonian but the expressions quoted here are more general than for the half-filled case). For nearest-neighbor hopping, we have the nesting property

$$\epsilon_{\mathbf{k}+\mathbf{Q}_d} = -\epsilon_{\mathbf{k}} \tag{A4}$$

that can be used to rewrite

$$\chi_0^R(\mathbf{Q}_d, \omega) = 2 \int dE N_d(E) \; \frac{1 - f(E+\mu) - f(E-\mu)}{\omega + i\eta + 2E} \tag{A5}$$

where $N_d(E)$ is the single-spin density of states for the given dimension.

In the limit $\mu \ll T$ we have for the static susceptibility

$$\chi_0(\mathbf{Q}_d) \equiv \chi_0^R(\mathbf{Q}_3, 0) = 2 \int dE N_d(E) \; \frac{1 - 2f(E)}{2E} \tag{A6}$$

so that in two dimensions $\chi_0(\mathbf{Q}_2) \sim \ln^2(t/T)$ while in three dimensions $\chi_0(\mathbf{Q}_3) \sim \ln(t/T)$. In the quasi two-dimensional case with $t_\parallel \ll T$ the two-dimensional value of χ_0 is an accurate approximation. The numerical values of $\chi_0(\mathbf{Q}_d)$ are in practice easy to obtain from numerical integrations.

For the microscopic relaxation time when $\mu \ll T$ we start from

$$\mathrm{Im}\, \chi_0^R(\mathbf{Q}_d, \omega) = \pi N_d(\frac{\omega}{2}) \tanh\left(\frac{\omega}{4T}\right). \tag{A7}$$

In two dimensions, the logarithmic divergence of the density of states $N_d(\frac{\omega}{2})$ at the van Hove singularity makes the zero-frequency limit of the microscopic relaxation time ill-defined. Nevertheless, van Hove singularities are usually washed out by lifetime effects in more self-consistent treatments so that one expects that for $\omega << T$ one has $\partial \chi_0^R(\mathbf{Q}_d,\omega)/d\omega\big|_{\omega=0} \sim 1/T$ leading to the temperature scaling of $\tau_0 \sim \left(T \ln T^{-1}\right)^{-1}$ in $d > 2$ described in the text.

We move on to evaluate analytically the wave vector derivatives in the regime $t_\parallel \ll T_N < T_X$. Keeping for a while a general notation where i is some direction (x, y, or z), one can write

$$\frac{\partial^2 \chi_0}{\partial q_i^2} = -8 t_i^2 a_i^2 \int_{BZ} \frac{d^3k}{(2\pi)^3} \frac{\partial^2 C}{\partial \epsilon_{\mathbf{k}+\mathbf{q}}^2} \; \sin^2(k_i + q_i) - 4 t_i a_i \int_{BZ} \frac{d^3k}{(2\pi)^3} \frac{\partial C}{\partial \epsilon_{\mathbf{k}+\mathbf{q}}} \cos(k_i + q_i), \tag{A8}$$

where

$$C(\epsilon_{\mathbf{k}+\mathbf{q}}, \epsilon_{\mathbf{k}}) = \frac{f(\epsilon_{\mathbf{k}+\mathbf{q}} - \mu) - f(\epsilon_{\mathbf{k}} - \mu)}{\epsilon_{\mathbf{k}+\mathbf{q}} - \epsilon_{\mathbf{k}}}.$$

Assuming $t_\parallel/T \ll 1$, we evaluate second derivatives to the lowest non-zero term in powers of $t_\parallel/T$. For $q_i = q_\parallel$, the leading term in Eq. (A8) gives a $t_\parallel^2$ contribution if we keep $t_\parallel = 0$ in the integrand. The second term gives also to leading order a quadratic contribution in $t_\parallel$. The spread of the Fermi factors over an energy interval of order T allows us to neglect all other dependencies in $t_\parallel$ and to perform the integral in the third direction trivially, enabling us to rewrite the remaining integral in terms of the two-dimensional single-spin density of states $N_2(E)$. After some algebra we get

$$\frac{\partial^2 \chi_0(\mathbf{Q}_{3D})}{\partial q_\parallel^2} = -2 t_\parallel^2 a_\parallel^2 \int_0^{4t} dE N_{2D}(E) \{ \frac{f'(E+\mu) + f'(E-\mu)}{E^2} + \frac{1 - f(E+\mu) - f(E-\mu)}{E^3} \} + O((\frac{t_\parallel}{T})^3) \tag{A9}$$

where f' is the derivative of the Fermi function. Using the expansion of Fermi functions and derivatives near $E = 0$, it can be shown that the integrand in the preceding equation is finite at finite temperature. Indeed as $E/T \to 0$, it behaves as $N_{2D}(E) f'''(\mu)$, where f''' is the third derivative of the Fermi function. At low temperature, approximating the integrand by $N_{2D}(E) f'''(\mu)$ over an energy interval T shows immediately that

$$\frac{\partial^2 \chi_0(\mathbf{Q}_{3D})}{\partial q_\parallel^2} \sim a_\parallel^2 \frac{t_\parallel^2}{T^2}. \tag{A10}$$

More precisely, $1/T^2$ should be multiplied by a logarithmic correction that comes from the $2D$ density of states. Numerical integration of (A9) shows that this $t_\parallel^2 \frac{1}{T^2}$ behavior occurs on a wider range of temperature than first expected: $T = 0.2t$ is already in this regime.

We can evaluate the in-plane $q_i = q_\perp$ derivative in the same spirit. This time take $t_\parallel = 0$ from the start since the leading order is in $t_\perp^2/T^2 \gg t_\parallel^2/T^2$. We thus have $\partial^2\chi_0(\mathbf{Q}_3)/\partial q_\perp^2 \approx \partial^2\chi_0(\mathbf{Q}_2)/\partial q_\perp^2$. After tedious algebra we finally get

$$\frac{\partial^2\chi_0(\mathbf{Q}_3)}{\partial q_\perp^2} \simeq t_\perp^2 a_\perp^2 \int_0^{4t} dE N_{2D}(E) \left\{ \frac{1}{2}\left[f'(E+\mu) + f'(E-\mu)\right] + \frac{1-f(E+\mu)-f(E-\mu)}{2E} \right\}$$

$$-t_\perp^2 a_\perp^2 \int_0^{4t} dE M(E) \left\{ \frac{1}{E}\left[f''(E+\mu) + f''(E-\mu)\right] \right.$$

$$\left. - \frac{f'(E+\mu)+f'(E-\mu)}{E^2} - \frac{1-f(E+\mu)-f(E-\mu)}{E^3} \right\}, \tag{A11}$$

where the integral

$$M(E) \equiv \int_{-\pi}^{\pi} dq_x 4\sin^2 q_x \int \frac{d^2k}{(2\pi)^2} \delta\left(E - \epsilon_{\mathbf{k}}\right) \delta\left(q_x - k_x\right) \tag{A12}$$

can be interpreted as an average over the surface of constant energy E of the square of the Fermi velocity in the x direction times the density of states at this energy. It can be evaluated analytically as

$$M(E) = \frac{2}{\pi^2}\{2\mathbf{E}(k^2) - \frac{E}{2t_\perp}(1+\frac{E}{2t_\perp})\mathbf{F}(k^2) + \frac{E^2}{4t_\perp^2}\mathbf{\Pi}(\alpha^2,k^2)\}. \tag{A13}$$

Here $\mathbf{F}(k^2)$, $\mathbf{E}(k^2)$ and $\mathbf{\Pi}(\alpha^2,k^2)$ are complete elliptic integrals of respectively first, second and third kinds, with $k^2 = 1 - E^2/\left(16t_\perp^2\right)$, and $\alpha^2 = 1 - E/\left(4t_\perp\right)$. Again at $E/T = 0$ the integrand in Eq.(A11) is well defined, and using Fermi function expansion it can be shown that at low temperature $\partial^2\chi_0(Q)/\partial q_\perp^2$ scales as $a_\perp^2 t_\perp^2/T^2$, with this time *no* logarithmic prefactor as before. More precisely we found numerically for a wide range of temperature (wider than the range studied in the main text) the following behavior

$$\frac{\partial^2\chi_0(\mathbf{Q}_e)}{\partial q_\perp^2} \simeq -0.085 a_\perp^2 \frac{t_\perp^2}{T^2} \tag{A14}$$

and correspondingly,

$$\left(\xi_0^\perp\right)^2 \equiv \frac{-1}{2\chi_0\left(\mathbf{Q}_d\right)} \left.\frac{\partial^2\chi_0\left(\mathbf{q},0\right)}{\partial q_\perp^2}\right|_{\mathbf{q}=\mathbf{Q}_d} \simeq 0.085 a_\perp^2 \frac{U_{mf,c}}{4}\frac{t_\perp^2}{T^2}.$$

From Eqs.(A10) and (A14) and a numerical evaluation of the corresponding quantities, one finds the following scaling

$$\frac{\xi_0^\parallel}{\xi_0^\perp} \simeq \frac{t_\parallel a_\parallel}{t_\perp a_\perp}. \tag{A15}$$

To conclude this appendix let us stress the fact that expanding $\chi_0(\mathbf{q} - \mathbf{Q}_{2D})$ to the second order using Eq. (A11) to obtain the asymptotic form of the $2D$-spin susceptibility is valid as long as the maximum of χ_0 is at (π,π), which is more general than half-filling. Indeed, by symmetry, the first derivative of the free susceptibility at $\mathbf{Q}_{2D}$ is zero for all fillings n and temperature and, as discussed before [26] [7], at finite temperature and away from half-filling the absolute maximum of the free susceptibility can be at (π,π) even if it is not the case at $T = 0$. This behavior can be observed in Figure 5 where the in-plane second derivative is plotted as a function of temperature for various values of band filling. When the second derivative goes to zero there is a shift in the wave vector maximizing the free susceptibility. Whether the magnetic transition will be commensurate or incommensurate at a given filling depends on the interaction U because by changing U one can change the ratio μ/T_X and because the nature of the final three-dimensional order depends very much at which wave vector correlations start to grow below T_X. [7]

Calculations presented along the above lines do not allow us to study the case where the maximum occurs at an incommensurate vector since we need the analytical expressions for the second derivatives of χ_0 to perform very accurate numerical calculations (When the wave vector $\mathbf{q}$ is different from (π,π) we do not have anymore the useful simplification: $\epsilon_{\mathbf{k}+\mathbf{q}} = -\epsilon_{\mathbf{k}}$ allowing us to replace the (k_x,k_y) integration in Eq.(A8) by a simpler integral on the $2D$ density of states.) Progress is nevertheless possible numerically within the TPSC approach.

APPENDIX B: ESTIMATES FOR $\widetilde{\sigma}^2$ AND Λ^{-1} IN THE NEARST-NEIGHBOR MODEL.

In this appendix we provide estimates for $\widetilde{\sigma}^2$ and Λ^{-1} in the isotropic two-dimensional nearest-neighbor model. The surprisingly low numerical values $\tilde{\sigma}^2 \simeq 0.21$, $\Lambda^{-1} \simeq 0.022$ obtained for $U = 4$ in the text are special to the Model C perfect nesting case.

We first rearrange the self-consistency equation Eq.(7) to isolate the asymptotic behavior, as we did in Eq.(39) but here in two dimensions and with $a_\perp = 1$.

$$n - 2\langle n_\uparrow n_\downarrow\rangle = T\int \frac{d^2q}{(2\pi)^2}\chi^{as}_{sp}(\mathbf{q},0) + T\int \frac{d^2q}{(2\pi)^2}\sum_{iq_n}\left[\chi_{sp}(\mathbf{q},iq_n) - \chi^{as}_{sp}(\mathbf{q},0)\,\delta_{n,0}\right]. \tag{B1}$$

It is usually assumed that the last integral on the right-hand side is weakly temperature dependent and it is included with the left-hand side to define $\widetilde{\sigma}^2$. This procedure usually suffices for reasons we will see below. For a more accurate estimate of $\widetilde{\sigma}^2$ close to T_X we use the Euler-Maclaurin formula to approximate the sum over Matsubara frequencies larger than the zeroth one by an integral. Recalling also that $\chi_{sp}(\mathbf{q},iq_n) = \chi_{sp}(\mathbf{q},-iq_n)$ we have

$$\begin{aligned} n - 2\langle n_\uparrow n_\downarrow\rangle = {} & T\int \frac{d^2q}{(2\pi)^2}\chi^{as}_{sp}(\mathbf{q},0) + T\int \frac{d^2q}{(2\pi)^2}\left[\chi_{sp}(\mathbf{q},0) - \chi^{as}_{sp}(\mathbf{q},0)\right] \\ & + T\int \frac{d^2q}{(2\pi)^2}\chi_{sp}(\mathbf{q},iq_1) + 2\int_{2\pi T}^{\infty}\frac{d\lambda}{2\pi}\int \frac{d^2q}{(2\pi)^2}\chi_{sp}(\mathbf{q},i\lambda). \end{aligned} \tag{B2}$$

To recast this result in the same form as the consistency condition Eq.(22), we first note that a more satisfactory definition of $\widetilde{\sigma}^2$ than the one given in Eq.(23) would be

$$\widetilde{\sigma}^2 = n - 2\langle n_\uparrow n_\downarrow\rangle - 2\int_{2\pi T}^{\infty}\frac{d\lambda}{2\pi}\int \frac{d^2q}{(2\pi)^2}\chi_{sp}(\mathbf{q},i\lambda). \tag{B3}$$

Also, the coefficient of the term linear in temperature on the right-hand side of Eq.(22) would not only include the asymptotic Lorentzian form but also a correction from the deviation to Lorentzian and another correction from the first Matsubara frequency. Overall then, a more accurate expression for the consistency condition is given by the last definition of $\widetilde{\sigma}^2$ and

$$\widetilde{\sigma}^2 = T\left\{\int \frac{d^2q}{(2\pi)^2}\chi^{as}_{sp}(\mathbf{q},0) + \int \frac{d^2q}{(2\pi)^2}\left[\chi_{sp}(\mathbf{q},0) - \chi^{as}_{sp}(\mathbf{q},0)\right] + \int \frac{d^2q}{(2\pi)^2}\chi_{sp}(\mathbf{q},iq_1)\right\}. \tag{B4}$$

The rest of this appendix is in two parts. We first estimate the left-hand side of this equation, $\widetilde{\sigma}^2$, and then we estimate the integrals on the right-hand side to obtain Λ^{-1}.

To obtain $\widetilde{\sigma}^2$, one should first notice that at the crossover temperature the local moment $n - 2\langle n_\uparrow n_\downarrow\rangle$ is already quite close to its zero-temperature value. Taking this as an estimate, we have

$$n - 2\langle n_\uparrow n_\downarrow\rangle = 2\int_0^{\infty}\frac{d\lambda}{2\pi}\int \frac{d^2q}{(2\pi)^2}\chi_{sp}(\mathbf{q},i\lambda) \tag{B5}$$

so that, substituting back into Eq.(B3), we have

$$\widetilde{\sigma}^2 = 2\int_0^{2\pi T}\frac{d\lambda}{2\pi}\int \frac{d^2q}{(2\pi)^2}\chi_{sp}(\mathbf{q},i\lambda). \tag{B6}$$

To estimate this integral for the case of perfect nesting , we note that singularities of $\chi_{sp}(\mathbf{q},0)$ near wave vectors $\mathbf{q} = 0$ and $\mathbf{q} = (\pi,\pi)$ are integrable singularities. We thus use the mean-value theorem to write, in our dimensionless units

$$\int \frac{d^2q}{(2\pi)^2}\chi_{sp}(\mathbf{q},i\lambda) \simeq \chi_{sp}(\mathbf{q}_{typ},i\lambda) \tag{B7}$$

As a representative point, one can take $\mathbf{q}_{typ} = (\pi,0)$ since it is far from both singularities. Using the trapezoidal rule to estimate the frequency integral, one has

$$\widetilde{\sigma}^2 \simeq 2\frac{2\pi T}{2\pi}\left[\frac{\chi_{sp}\left(\mathbf{q}_{typ},0\right)+\chi_{sp}\left(\mathbf{q}_{typ},2\pi T\right)}{2}\right]\simeq 0.19 \tag{B8}$$

whose numerical value follows from results obtained for $U=4$, $T_X\simeq 0.2$, $U_{sp}\simeq U_{mf,c}\simeq 2$,

$$\begin{aligned}\chi_{sp}\left(\mathbf{q}_{typ},0\right) &\simeq 0.60\\ \chi_{sp}\left(\mathbf{q}_{typ},2\pi T_x\right) &\simeq 0.36.\end{aligned} \tag{B9}$$

The estimated numerical value of $\widetilde{\sigma}^2$ in Eq.(B8) corresponds closely to the value obtained in the text from accurate numerical solutions. The fact that $\widetilde{\sigma}^2$ scales roughly as $T_X\sim T_{mf,c}$ in very weak coupling, as follows from Eq.(B8), is a significant result since $\widetilde{\sigma}^2$ is also related to the size of the pseudogap between precursors of antiferromagnetic bands, as shown in Ref. [13].

To estimate the value of Λ^{-1}, we notice that in the usual consistency condition Eq.(22), one keeps only the first term on the right-hand side of the more accurate expression Eq.(B4). The effect of the other terms is mimicked by using an effective cutoff Λ that is not equal to the Brillouin zone size, as one might have naively expected. In other words, the effective cutoff Λ may be obtained by requiring that

$$\int_0^{\Lambda}\frac{qdq}{2\pi}\chi_{sp}^{as}\left(\mathbf{q},0\right)=\int_0^{\pi}\frac{qdq}{2\pi}\chi_{sp}^{as}\left(\mathbf{q},0\right)+\int\frac{d^2q}{\left(2\pi\right)^2}\left[\chi_{sp}\left(\mathbf{q},0\right)-\chi_{sp}^{as}\left(\mathbf{q},0\right)\right]+\int\frac{d^2q}{\left(2\pi\right)^2}\chi_{sp}\left(\mathbf{q},iq_1\right). \tag{B10}$$

When there is no nesting, the quantity ξ_0 is relatively small at the crossover temperature, meaning that the asymptotic Lorentzian form is not so peaked and should be a good estimate of the susceptibility over much of the Brillouin zone. Because of the slow decay of the asymptotic form $\chi_{sp}^{as}\left(\mathbf{q},0\right)$, the second integral should in fact be negative and should partly cancel the last integral so that we should have $\Lambda\sim\pi$. By contrast, for perfect nesting $\xi_0\sim 1/T$ is large, as seen in Appendix A, meaning that in this case the asymptotic form $\chi_{sp}^{as}\left(\mathbf{q},0\right)$ is valid only in a narrow range of $\mathbf{q}$ values. Over most of the Brillouin zone, away from the maximum, the true susceptibility $\chi_{sp}\left(\mathbf{q},0\right)$ is larger than the asymptotic one $\chi_{sp}^{as}\left(\mathbf{q},0\right)$ because the latter decays rapidly away from the maximum while the true one has an extremum at both the Brillouin zone corner and center. The same arguments as those used to evaluate integrals for $\widetilde{\sigma}^2$ allow us then to estimate

$$\int\frac{d^2q}{\left(2\pi\right)^2}\left[\chi_{sp}\left(\mathbf{q},0\right)-\chi_{sp}^{as}\left(\mathbf{q},0\right)\right]\simeq\chi_{sp}\left(\mathbf{q}_{typ},0\right)\simeq 0.60 \tag{B11}$$

$$\int\frac{d^2q}{\left(2\pi\right)^2}\chi_{sp}\left(\mathbf{q},iq_1\right)\simeq\chi_{sp}\left(\mathbf{q}_{typ},2\pi T_x\right)\simeq 0.36 \tag{B12}$$

so that the equation Eq.(B10) that determines the cutoff becomes, with $U_{sp}\simeq 2$ and $\xi_0^2\left(T_X\right)\simeq 1$,

$$\int_{\pi}^{\Lambda}\frac{qdq}{2\pi}\chi_{sp}^{as}\left(\mathbf{q},0\right)=\int_{\pi}^{\Lambda}\frac{qdq}{2\pi}\frac{2}{U_{sp}\xi_0^2}\frac{1}{\xi^{-2}+\mathbf{q}^2}\simeq 0.96 \tag{B13}$$

$$\Lambda^{-1}=\pi^{-1}\exp\left(-\frac{\pi U_{sp}\xi_0^2}{2}0.96\right)\simeq 0.016. \tag{B14}$$

Although the difference with the numerically accurate result seems relatively large, one should really compare the estimates of $\ln\Lambda^{-1}$. The above estimate, $\ln 0.016\simeq -4.1$, differs only by roughly 10% from the estimate, $\ln 0.022=-3.8$, obtained from a logarithmic plot of the numerically accurate solution.

APPENDIX C: EXACT RESULT FOR $\int D^3Q\chi_{SP}^{AS}$

In this appendix we find the integral of the asymptotic part of the spin susceptibility near $\mathbf{Q}_3=(\pi,\pi,\pi)$. Let $\chi_{as}(\mathbf{q}+\mathbf{Q}_3,0)$ be the approximate spin susceptibility near $\mathbf{Q}_3$ obtained in Eq.(40) with $q_{\perp}^2=q_x^2+q_y^2$ and $q_{\parallel}=q_z$ First we integrate in the z-direction from $-\Lambda_{\parallel}$ to $\Lambda_{\parallel}$, with $\Lambda_{\parallel}=\pi/a_{\parallel}$, then change to polar coordinates in the plane and integrate on a circle of radius $\Lambda_{\perp}$ to finally obtain

$$\int_D\frac{d^3q}{\left(2\pi\right)^3}\chi_{sp}^{as}(\mathbf{q}+\mathbf{Q}_3,0)=\frac{1}{\pi U_{sp}\left(\xi_0^{\perp}\right)^2 a_{\parallel}}\left[-\frac{1}{\Lambda_{\parallel}\xi_{\parallel}}\mathrm{arctg}\Lambda_{\parallel}\xi_{\parallel}\right.$$

$$+\frac{1}{\Lambda_{\parallel}\xi_{\parallel}}\sqrt{1+\Lambda_{\perp}^{2}\xi_{\perp}^{2}}\ \mathrm{arctg}\frac{\Lambda_{\parallel}\xi_{\parallel}}{\sqrt{1+\Lambda_{\perp}^{2}\xi_{\perp}^{2}}}+\frac{1}{2}\ \ln(1+\frac{\Lambda_{\perp}^{2}\xi_{\perp}^{2}}{1+\Lambda_{\parallel}^{2}\xi_{\parallel}^{2}})\Bigg]. \tag{C1}$$

This analytical result provides another route to obtain the Néel temperature and the $d=2$ to $d=3$ crossover as discussed in the following section.

APPENDIX D: EXTENDED SCALING HYPOTHESIS AND UNIVERSALITY FOR THE RENORMALIZED-CLASSICAL $D=2$ TO $D=3$ CROSSOVER.

We first briefly recall the results of Ref. [27] on universality of crossover scaling functions in anisotropic systems. The discussion usually centers on anisotropy in spin space rather than position space but the results are generally applicable. Suppose one has a very small anisotropy g. Sufficiently far from the transition, the critical behavior will be that of the isotropic fixed point and should be described by the *extended scaling hypothesis* for the singular part of the free energy density. The same extended scaling hypothesis follows for other thermodynamic response functions. We use the symbol ($\approx$) to mean "asymptotically equal to" and ($\sim$) to mean "scales as". Let us concentrate on the magnetic susceptibility

$$\chi(g,t)\approx At^{-\gamma}X\left(Bg/t^{\phi}\right) \tag{D1}$$

where

$$t\equiv\left(\frac{T-T_{c}(0)}{T_{c}(0)}\right) \tag{D2}$$

with ϕ the crossover exponent and $T_c(0)$ the value of the transition temperature at zero anisotropy $g=0$. It is clearly the large value of the correlation length that validates the scaling hypothesis. The scale factors A and B in Eq.(D1) are non-universal, but the scaling function is. The value of A for a given model is fixed by the normalization condition $X(0)=1$.

Near the true transition temperature at the anisotropic fixed point, the susceptibility should obey the usual result

$$\chi(g,t)\approx\dot{A}(g)\ \dot{t}^{-\dot{\gamma}} \tag{D3}$$

where quantities with a dot refer to properties of the anisotropic fixed point, and

$$t(T,g)=\left(\frac{T-T_{c}(g)}{T_{c}(0)}\right)+\left(\frac{T_{c}(g)-T_{c}(0)}{T_{c}(0)}\right)=\dot{t}+t_{c}(g). \tag{D4}$$

The two expressions for the susceptibility Eqs.(D1) and (D3) are consistent only if the crossover scaling function $X\left(Bg/t^{\phi}\right)$ is singular as a function of its argument, namely

$$\lim_{x\to x_{c}}X(x)=X_{0}\left(1-\frac{x}{x_{c}}\right)^{-\dot{\gamma}} \tag{D5}$$

where X_0 is a universal amplitude while x_c is a g and t independent universal number. The definition

$$x=Bg/\left(t(g)\right)^{\phi} \tag{D6}$$

immediately implies that the transition temperature is at

$$t_{c}(g)=\left(Bg/x_{c}\right)^{1/\phi}. \tag{D7}$$

The generalization to the $d=2$ to $d=3$ crossover is not completely trivial because in $d=2$ the correlation length is not a power law of temperature for $O(n)$ models with $n>1$. Fisher and Barber [24] in their study of crossover in helium films have considered the case where the system is three-dimensional at high temperature and two-dimensional at low temperature, opposite to the situation we consider. Furthermore, the transition temperature is finite in $d=2$ helium films. Kosterlitz and Santos [22] did consider the case of interest here, both within a one-loop renormalization group approach, and in the spherical model. To cast the results of the latter paper in the language of the extended scaling hypothesis, it suffices to recall the usual hypothesis that the divergence of the correlation length in the plane is

at the origin of the scaling behavior. Hence, $t\left(T\right)^{-\nu}$ can be replaced everywhere in the above equations by a function of absolute temperature that scales with T in the same way as the two-dimensional correlation length [28]

$$\xi_{2d}\left(T\right) \equiv T^{a}\exp\left(C/T\right). \tag{D8}$$

In this expression, we have allowed for a possible algebraic preexponential factor. For example, to one loop order [22] in the momentum-shell method [29] the preexponential factor is $a = \left(n-2\right)^{-1}$ while to two-loop order [30] as well as in the $n \to \infty$ limit, only the exponential is present, $a = 0$. In addition to the non-universal quantities A and B defined above, we now have an additional non-universal constant C in Eq.(D8). This is not fundamentally different from the usual case where the relation between t and absolute temperature also involves a non-universal constant, namely $T_c\left(0\right)$. The only difference between the itinerant case and the usual $n-$vector model is that C can be temperature dependent in the case of nesting, as discussed in the text and in Appendix A. When there is no nesting symmetry, C is temperature independent. In the strong-coupling limit, one usually defines $C = 2\pi\rho_S$.

With the above $t\left(T\right)^{-\nu} \to \xi_{2d}\left(T\right)$ hypothesis, the extended scaling hypothesis becomes

$$\chi^{R}_{sp}(\mathbf{Q}_d,0) \approx A\xi_{2d}^{\gamma/\nu}X\left(Bg\xi_{2d}^{\phi/\nu}\right) \tag{D9}$$

where $g = \left(t_{\parallel}/t_{\perp}\right)^{2}$ plays the role of the anisotropy parameter in the case we have considered in detail in the text. The function $X\left(x\right)$ is a universal function that we normalize to $X\left(0\right) = 1$. With precisely the same asymptotic form as in Eq.(D5), simple power series expansion in powers of $T - T_N$ allows one to recover the correct critical behavior near the three-dimensional Néel temperature. Hence, the Néel temperature is given by $x_c = B\left(t_{\parallel}/t_{\perp}\right)^{2}\xi_{2d}^{\phi/\nu}$ so that with the $n \to \infty$ result $\phi/\nu = \gamma/\nu = 2$ and Eq.(D8) one recovers the result of the main text

$$\frac{C}{T_N} \sim \ln\left(\frac{t_{\perp}}{t_{\parallel}}\right)^{2} \tag{D10}$$

with C taking its appropriate temperature-dependent value in the nesting case.

We conclude by an explicit calculation of the universal crossover function for the staggered susceptibility in the $n \to \infty$ limit. In this case, $a = 0$ in Eq.(D8). The general form of the susceptibility is given by Eq.(15) with $\xi^2 = \xi_0^2\left(U_{sp}/\delta U\right)$

$$\chi^{R}_{sp}(\mathbf{Q}_d,0) \approx \frac{2}{\delta U}. \tag{D11}$$

The value of δU is in turn obtained by solving the self-consistency condition Eq.(39)

$$\widetilde{\sigma}^2 = Ta_{\parallel}a_{\perp}^{2}\int\frac{d^3q}{\left(2\pi\right)^3}\chi^{as}_{sp}\left(\mathbf{q},0\right) \tag{D12}$$

where $\widetilde{\sigma}^2$ takes essentially its $d = 2$ value with very small corrections. We can use the result of the previous appendix Eq.(C1) for the integral. It is then convenient to rewrite the result of the integral in terms of the following dimensionless variables

$$\alpha \equiv \frac{\Lambda_{\parallel}^{2}\xi_{\parallel}^{2}}{\Lambda_{\perp}^{2}\xi_{\perp}^{2}} = \frac{\Lambda_{\parallel}^{2}\left(\xi_0^{\parallel}\right)^{2}}{\Lambda_{\perp}^{2}\left(\xi_0^{\perp}\right)^{2}} = cst\left(\frac{t_{\parallel}}{t_{\perp}}\right)^{2} \tag{D13}$$

$$u \equiv \Lambda_{\parallel}\xi_{\parallel} = \Lambda_{\parallel}\xi_0^{\parallel}\left(U_{sp}/\delta U\right)^{-1/2}. \tag{D14}$$

Since we assume that we are in the scaling regime, namely the one where the two-dimensional correlation length is very large, $\left(\Lambda_{\perp}^{2}\xi_{\perp}^{2}\right) \gg 1$, we can use

$$\alpha \ll u^2 \tag{D15}$$

to expand Eq.(C1) and write

$$\frac{\pi U_{sp}\left(\xi_0^{\perp}\right)^{2}\widetilde{\sigma}^2}{Ta_{\perp}^{2}} = \ln\alpha^{-1/2} + \ln\left(\frac{u^2}{u^2+1}\right)^{1/2} + 1 - \frac{1}{u}\arctan\left(u\right). \tag{D16}$$

If one solves the above implicit equation for u, then the susceptibility Eq.(D11) follows immediately from u^2 in Eq.(D14) since

$$\chi_{sp}^{R}(\mathbf{Q}_d,0) = \frac{2u^2}{\Lambda_{\|}^2 \left(\xi_0^{\|}\right)^2 U_{sp}}. \tag{D17}$$

Note that u is a function of the dimensionless quantity x defined by

$$x \equiv \alpha \xi_{2d}^2 = \alpha \exp\left(2C/T\right) = \alpha \Lambda_{\perp}^2 \xi_{\perp}^2 \tag{D18}$$

$$C \equiv \frac{\pi U_{sp} \left(\xi_0^{\perp}\right)^2 \widetilde{\sigma}^2}{a_{\perp}^2} \tag{D19}$$

as may be seen by exponentiating the implicit equation Eq.(D16)

$$x = \left(\frac{u^2}{1+u^2}\right) \exp\left(2 - \frac{2}{u} \arctan u\right). \tag{D20}$$

Before explicitly solving this equation in limiting cases, let us express the universal scaling function X in terms of u. The last equation for the susceptibility Eq.(D17) may be rewritten with the above definitions as

$$\chi_{sp}^{R}(\mathbf{Q}_d,0) = \frac{2u^2\left(x\right)}{\alpha \Lambda_{\perp}^2 \left(\xi_0^{\perp}\right)^2 U_{sp}} = A \xi_{2d}^2 X\left(x\right) = \frac{2\xi_{\perp}^2}{\left(\xi_0^{\perp}\right)^2 U_{sp}} X\left(x\right) \tag{D21}$$

where

$$X\left(x\right) \equiv \frac{u^2\left(x\right)}{x} \tag{D22}$$

and

$$A \equiv \frac{2}{\Lambda_{\perp}^2 \left(\xi_0^{\perp}\right)^2 U_{sp}}. \tag{D23}$$

The universal crossover function $X\left(x\right)$ is plotted in Fig.6. Let us check various limiting forms analytically. This will allow us to recover all the cases studied in the main body of the paper. First, the two-dimensional limit is the one where $u \to 0$. In this limit, the implicit equation (D20) reduces to $x = u^2$. This verifies that we have the proper normalization $X\left(x\right) = 1$. The three-dimensional limit is the limit where $u^2 \to \infty$. In this limit,

$$x_c = e^2. \tag{D24}$$

Keeping the next term in the $1/u$ expansion, we have

$$\lim_{x \to x_c} X\left(x\right) = \left(\frac{\pi}{e}\right)^2 \left(1 - \frac{x}{x_c}\right)^{-2} \tag{D25}$$

hence the universal constant X_0 takes the value $\left(\pi/e\right)^2$. As expected the susceptibility exponent in $d = 3$ is $\dot{\gamma} = 2$. The Néel temperature follows from

$$x_c = \alpha \exp\left(2C/T_N\right) \tag{D26}$$

or

$$\frac{C}{T_N} = \ln\left(\frac{e\Lambda_{\perp}\xi_{\perp}}{\Lambda_{\|}\xi_{\|}}\right) \sim \ln\left(\frac{t_{\perp}}{t_{\|}}\right). \tag{D27}$$

Finally, the $d = 2$ to $d = 3$ crossover temperature is given by $u = \Lambda_{\|}\xi_{\|} = 1$. Obviously, the criterion $\Lambda_{\|}\xi_{\|} = 1$ is subjective. We could take $\Lambda_{\|}\xi_{\|}$ to be equal to any other finite number. For definiteness however, we continue with $\Lambda_{\|}\xi_{\|} = 1$. Substituting in Eq.(D20) we have $x^* = \frac{1}{2}\exp\left(2 - \frac{\pi}{2}\right)$ hence the crossover temperature T^* is given by

$$x^* = \alpha \exp\left(2C/T^*\right) \tag{D28}$$

Comparing with the equation for the Néel temperature Eq.(D26) we find that the scaling of $\exp\left(C/T^*\right)$ with the anisotropy parameter α is the same as that of $\exp\left(C/T_N\right)$. More specifically, we find, in agreement with the main text, Eq.(57), that the size of the crossover region is given by,

$$\left(1 - \frac{T_N}{T^*}\right) = \frac{T_N}{2C} \ln\left(x_c/x^*\right) = \frac{\ln\left(x_c/x^*\right)}{\ln \xi_{2d}\left(T_N\right)} = \log_{\xi_{2d}(T_N)}\left(x_c/x^*\right). \tag{D29}$$

In other words, the size of the crossover region, calculated in reduced temperature, decreases with T_N.

To complete the relation with the general functional form Eq.(D9) postulated above, note that if

$$g \equiv \left(\frac{t_\parallel}{t_\perp}\right)^2 \tag{D30}$$

then $x = Bg\xi_{2d}^{\phi/\nu} = \alpha\xi_{2d}^2$ with $\phi/\nu = 2$ implies that $B = \alpha/g$ is a number

$$B \equiv \frac{\Lambda_\parallel^2 \xi_\parallel^2}{\Lambda_\perp^2 \xi_\perp^2} \left(\frac{t_\perp}{t_\parallel}\right)^2 \tag{D31}$$

that is independent of g because of the scaling $\Lambda_\parallel^2\xi_\parallel^2/\ \Lambda_\perp^2\xi_\perp^2 \sim \left(t_\parallel/t_\perp\right)^2$ that follows from Appendix A, Eq.(A15).

The universal crossover scaling function beyond $n = \infty$ where the exponents ϕ/ν and γ/ν differ has yet to be investigated.

---

[1] S. Chakravarty, B.I. Halperin, and D.R. Nelson, Phys. Rev. B **39**, 2 344 (1989)..
[2] Subir Sachdev, Andrey V. Chubukov, and Alexander Sokol, electronic archives cond-mat/9411066
[3] Andrey V. Chubukov, Subir Sachdev, and Jinwu Ye, Phys. Rev. B **49**, 11 919 (1994).
[4] J.A. Hertz, Phys. Rev. B **14**, 1165 (1976).
[5] A.J. Millis, Phys. Rev. B **48**, 7183 (1993).
[6] For a review, see T. Moriya, *Spin Fluctuations in Itinerant Electron Magnetism*, Springer-Verlag, 1985.
[7] Y.M. Vilk, Liang Chen, A.-M.S. Tremblay, Phys. Rev. B **49**, 13 267 (1994).
[8] A. Veilleux, Liang Chen, Anne-Marie Daré, Y.M. Vilk, and A.-M.S. Tremblay, electronic archives, cond-mat/9507045.
[9] R. Konno, Prog. Theor. Phys. **87**, 1335 (1992).
[10] C. Bourbonnais and L.G. Caron, Int. J. Mod. Phys. B **5**, 1033 (1991); C. Bourbonnais and L.G. Caron, Europhys. Lett. **5,** 209 (1988); Physica B **143,** 451 (1986).
[11] Daniel Boies, C. Bourbonnais and A.-M.S. Tremblay, Phys. Rev. Lett. **74**, 968 (1995).
[12] B. Keimer, N. Belk, R.J. Birgeneau, A. Cassanho, C.Y. Chen, M. Greven, M.A. Kastner, A. Aharony, Y. Endoh, R.W. Erwin, G. Shirane, Phys. Rev. B **46**, 14 034 (1992).
[13] Y.M. Vilk and A.-M.S. Tremblay, Europhys. Lett. (in press).
[14] N.E. Bickers and D.J. Scalapino, Annals of Physics, **193**, 206 (1989).
[15] Pierre Bénard, Liang Chen and A.-M.S. Tremblay Phys. Rev. B **47**, 15 217 (1993).
[16] H.E. Stanley, in *Phase transitions and critical phenomena* (Oxford University Press, Oxford, 1971)
[17] Pierre Pfeuty and Gérard Toulouse, *Introduction to the Renormalization group and to Critical Phenomena (Wiley, London, 1977)* p.103
[18] In the practical situations discussed in the comparisons with experiment, we have that ξ varies between 1 and 1500 when the temperature varies between $0.16t$ and $0.2t$ so that the difference between $1/T$ and $1/T^3$ scaling is not so important in the accessible regime of temperatures.
[19] C.M. Soukoulis, D. Sreela and H.L. Young , Phys. Rev. B.**44**, 446, (1991).?
[20] Ravi P. Singh, Z.C. Tao, and M. Singh, Phys. Rev. B **46**, 1244 (1992).
[21] Avinash Singh, Zlatko Tešanović, H. Tang, C.L. Chien, J.C. Walker, Phys. Rev. Lett. **64**, 2571 (1990).
[22] J.M. Kosterlitz and M.A. Santos, J. Phys. C. **11**, 2835 (1978).
[23] E. Riedel, and F. Wegner, Z. Physik **225**, 195 (1969).
[24] M.E. Fisher and M.N. Barber, Phys. Rev. Lett. **28**, 1516 (1972).
[25] A.-M. Daré, PhD thesis, Université de Sherbrooke, 1994.

[26] H.J. Schulz, Phys. Rev. Lett. **64**, 1445 (1990).
[27] P. Pfeuty, D. Jasnow, and M.E. Fisher, Phys. Rev. B **10**, 2088 (1974).
[28] In cases where the two-dimensional correlation length has a power law prefactor, one should use $\xi_{2d}(T) = (T/T_0)^a \exp(C/T)$ where the value of T_0 is determined by a normalization condition that we are free to choose. We can choose $\xi_{2d}(T=1) = 1$ for example. Once this normalization is chosen, the non-universal quantities have a well defined value for any given model.
[29] D.R. Nelson and R.A. Pelcovits, Phys. Rev. B **16**, 2191 (1977).
[30] S. Chakravarty, B.I. Halperin, and D.R. Nelson, Phys. Rev. B **39**, 2344 (1989).

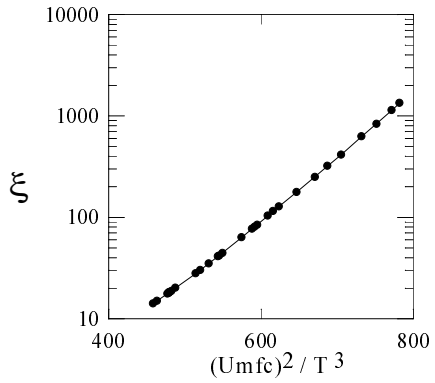

FIG. 1. Semi-logarithmic plot of the two-dimensional correlation length, showing the scaling as a function of temperature in the case of nesting.

Fig. 2

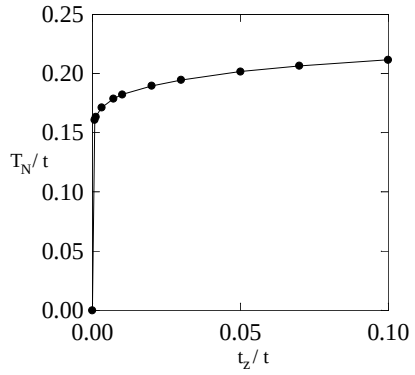

FIG. 2. Néel Temperature as a function of $t_z \equiv t_\parallel$ for $U = 4t_\perp$, at half-filling.

Fig. 3

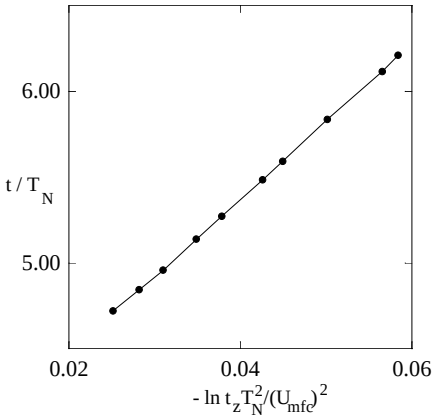

FIG. 3. $\frac{1}{T_N}$ as a function of $\frac{T_N^2}{U_{mfc}^2}\left|\ln\frac{t_z}{t}\right|$ for $U = 4t_\perp$ at half-filling. The quantities T and $t_z \equiv t_\parallel$ are in units of $t_\perp = t$.

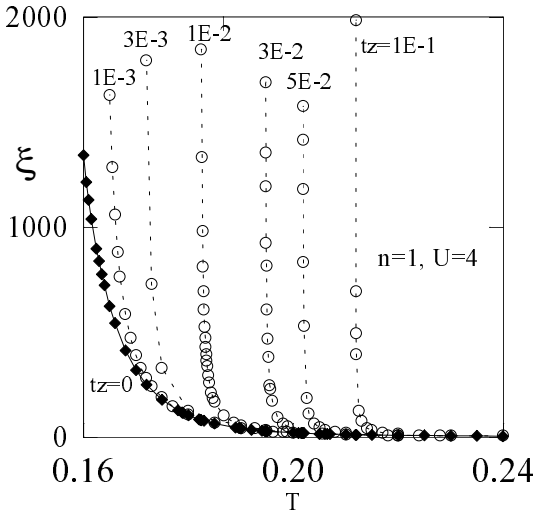

FIG. 4. In-plane correlation length $\xi_\perp$ (lattice space is unity) for several values of out-of-plane hopping parameter at half filling for $U = 4t_\perp$. T and $t_z \equiv t_\parallel$ are in units of $t_\perp$.

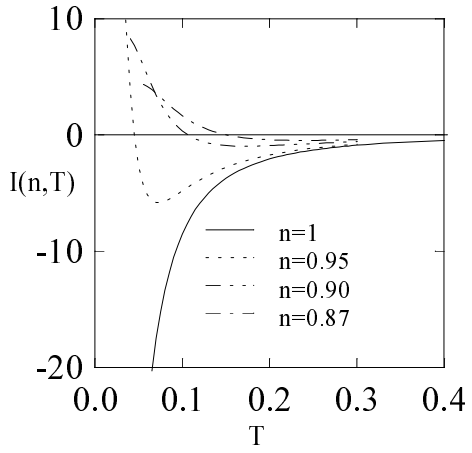

FIG. 5. Second in-plane derivative of the non-interacting susceptibility $I\left(n,T\right)=\partial^{2}\chi_{0}\left(\mathbf{q},0\right)/\partial^{2}q_{\perp}|_{\mathbf{Q}}$ in two-dimensions as a function of temperature for various band-fillings n.

Fig. 6

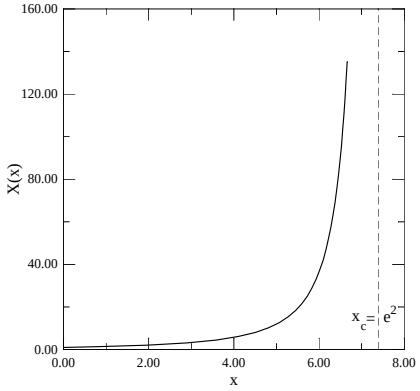

FIG. 6. Plot of the universal crossover function from $d=2$ to $d=3$ for the staggered susceptibility in the $n\rightarrow\infty$ limit as defined by Eqs.(D22) and (D20).